Volume 17, Issue 1, 172503 (1-10)

Iranian Journal of Earth Science (IJES)

https://dx.doi.org/10.57647/j.ijes.2025.1701.03

Landslide susceptibility mapping (LSM) of the Boudinar basin (Morocco) using the geographic information system (GIS) and the analytical hierarchy process (AHP) method

Morad Taher[1]*, Taoufik Mourabit[2], Hajar El Talibi[1], Afaf Amine[3], Abdelhak Bourjila[4], Ali Errahmouni[2], Sadik Azzouzi[6], Issam Etebaai[1]

[1]*Applied Geosciences and Geological Engineering Research Team, FSTH, Abdelmalek Essaâdi University, Tetouan, Morocco.*
[2]*Department of Geology, Faculty of Science, Abdelmalek Essaâdi University, Tetouan, Morocco.*
[3]*Geosciences, water and Environment Laboratory, Department of Geology, Faculty of Sciences, Mohammed V University in Rabat, Rabat, Morocco.*
[4]*Laboratory of Engineering Sciences and Applications (LSIA), Materials Science, Energy and Environment (SM2E), ENSAH, Abdelmalek Essaâdi University, Tetouan, Morocco.*
[5]*Department of Geography, The Faculty of Letters and Human Sciences of Oujda, Mohammed first University, Oujda, Morocco.*

*Corresponding author: m.taher@uae.ac.ma

Review Paper

Received:
19 April 2024
Revised:
7 May 2024
Accepted:
15 July 2024
Published online:
10 January 2025

Abstract:

Creating a landslide susceptibility map for the Boudinar basin is of paramount significance due to the region's susceptibility to landslides, which pose considerable risks to both human settlements and the environment. By integrating Geographic Information Systems (GIS) and the Analytical Hierarchy Process (AHP), our study aims to address this challenge. These methods provide distinct advantages, as they facilitate spatial analysis and enable a thorough evaluation of the various factors contributing to landslide susceptibility. Therefore, various factors were considered in the study, including rainfall, lithology, slope, aspect, NDVI, distance from the fault, distance from the river, distance from the road, and elevation. The causative factors were divided into sub-factors, and weightages were assigned based on the AHP methodology. The resulting landslide susceptibility map was classified into three categories: low (5 %, 18 km^2), moderate (69 %, 242 km^2), and high (25 %, 88 km^2). Nevertheless, the primary sources of uncertainty of our analysis include data quality, and the absence of field landslide inventory data for the validation process. Using Google Earth pro, the landslide inventory, consisting of 100 landslides, was used to validate the landslide susceptibility map, which had a prediction rate of 65.7% using the area under curve (AUC) technique. The LSM study is a valuable tool for construction planners and decision-makers. Therefore, by identifying high-risk areas, it aids in better preparedness and risk reduction efforts. Its integration into the planning process can significantly enhance the region's resilience to landslide hazards.

Keywords: Geological hazard; Heavy rainfall; Rif; Seismic activities

1. Introduction

Landslides pose significant risks to human life and economic growth worldwide (Reichenbach et al., 2018). These geological events described as a masses of earth, rock, or debris pulled downward by gravity (Akbar et al., 2022). The occurrence of earth moving could be associated with natural hazards or anthropogenic activities (Akbar et al., 2022; Leonardi et al., 2022; Hashemi et al., 2023). Natural phenomena include changes in the weather, such as prolonged or heavy rain or snowfall, as well as earthquakes and volcanic eruptions. On the other hand, human disruptions encompass changing land use, deforestation, excavation, altering slopes, and constructing infrastructure (Leonardi et al., 2022).

The mountainous areas of northern Morocco suffer greatly from landslide hazards. Additionally, the eastern regions of Al-Hoceima and Driouch are known for being tectonically active (Taher and Mourabit, 2022), while the western areas of Tanger, Tetouan, and Chefchaouen experience significant

precipitation. As a result, there are several major factors contributing to landslides in the Rif region, including the fragile lithology, such as shale. According to the field survey conducted by the Moroccan Provincial Directorate of Practical Work (PDOW), the Chefchaouen province witnessed 47 landslides until 1992, Tanger experienced 17 landslides, Tetouan had 19 landslides, and Al-Hoceima had one landslide (Fig. 1) (Himmi, 1994). Nowadays, the number of landslides in these provinces remains significant. For example, in Al-Hoceima alone, 151 landslides were identified during the period of 2004-2016 (Golian et al., 2021; Byou, 2021). Consequently, infrastructures such as roads, bridges, and human settlements are at risk due to landslide hazards. Creating a landslide susceptibility map is crucial for identifying potential preventive actions to minimize the damage and casualties. Landslide Susceptibility Mapping (LSM) is a geospatial analysis and modeling technique used to assess and predict the likelihood of landslides occurring in a specific area. It aims to identify and map areas that are more prone to landslides based on various geological, topographical, and environmental factors (Sun et al., 2023). Nowadays, the advancement of remote sensing (RS) and geographic information system (GIS) techniques has helped to classify different triggering factors of landslides and prepare a landslide inventory map (Gupta et al., 2022; Saadat et al., 2023). The generation, management, and analysis of geographic data, including forecasting potential landslide hazards, have been extensively carried out using the GIS (KC et al., 2022). Various GIS-based techniques have been employed for landslide susceptibility mapping (LSM), such as Analytical Hierarchy Processes (AHP) (Arjmandzadeh et al., 2017; Afzal et al., 2022; Agrawal and Dixit, 2022; Panchal and Shrivastava, 2020, 2022), the Frequency Ratio model (FR) (Liu et al., 2022; Sheng et al., 2022), and machine learning (ML) (Chang et al., 2022b; Trinh et al., 2022). Geospatial information on LSM can be beneficial in policymaking and management decision-making to mitigate and reduce the risks associated with landslide (Azarafza et al., 2021; Panchal and Shrivastava, 2021).

In recent years, much research has focused on landslide susceptibility in Al-Hoceima and the surrounding RIF region (Byou, 2021; Rahali, 2019). Accordingly, numerous tourist or commercial sites in the Al-Hoceima province have been threatened by landslides (Fig. 2a, b). On other hand, other

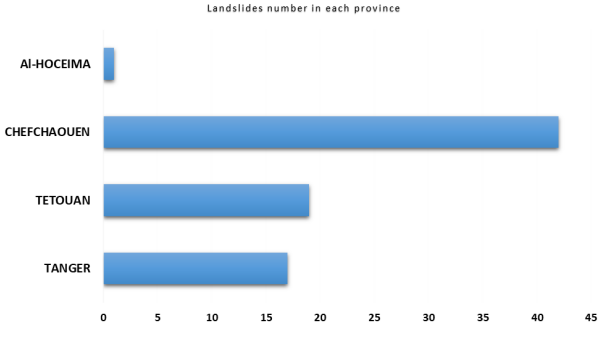

Figure 1. Landslides number of some provinces in North Morocco according to PDOW (Himmi, 1994).

Figure 2. a) Landslide on national road 2. b) Landslide on Corniche Sabadia. c: Retaining walls in the Al-Hoceima entrance. d) Rockfall Netting near to the Al-Hoceima port. © TAHER MORAD 2023.

sites have been protected from landslides through the implementation of retaining walls or rockfall netting (Fig. 2c, d). However, the landslide susceptibility of the northeastern Rif region, especially the Boudinar basin, has not received much attention. In this context, this study aims to integrate GIS and RS to create a LSM of the Boudinar basin, identify areas more prone to landslides, and determine the most important factors that can trigger landslides. To achieve these objectives, we identified nine factors that can trigger landslides: slope, aspect, NDVI, distance from faults, distance from roads, distance from river, lithology, rainfall, and altitude. The nine factors utilized in our study have not been previously employed simultaneously in AHP method, as indicated in the Table 1. However, it is worth noting that He et al. (2019) have employed all these factors, albeit in conjunction with different variables. The AHP method was employed to address the uncertainty and decisional imprecision associated with this study. By applying these techniques, a LSM was generated for the Boudinar basin, which was subsequently classified into three zones: low, moderate, and high susceptibility.

2. Study area

The Driouch province in northeastern Morocco (Fig. 3) encompasses the Boudinar basin, which comprises seven

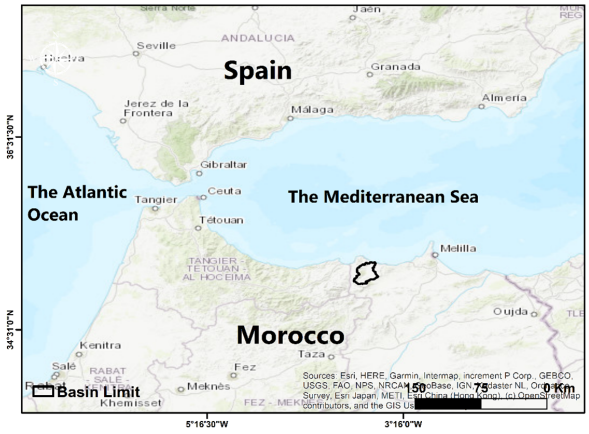

Figure 3. The geographic location of the Boudinar basin.

Table 1. The factors employed in previous studies using the AHP method.

	Altitude	Dis.f. Fault	Aspect	NDVI	Rainfall	Lithology	Dis.f.River	Dis.f.Roads	Slope
(Ibrahim et al., 2022)	✓		✓		✓	✓			✓
(Leonardi et al., 2022)	✓				✓	✓	✓	✓	✓
(Panchal and Shrivastava, 2022)		✓	✓			✓		✓	✓
(He et al., 2019)	✓	✓	✓	✓	✓	✓	✓	✓	✓
(Jazouli et al., 2019)	✓	✓	✓				✓	✓	✓
(Panchal and Shrivastava, 2021)			✓			✓		✓	✓
(Hamdouni et al., 2022)	✓		✓			✓			✓
(Seddiki and Dehimi, 2022)		✓				✓	✓	✓	✓
(Trisnawati et al., 2022)		✓			✓	✓			✓

rural municipalities, including Temsaman and Boudinar, that are significant in the region. The GIS-based delineation of the basin covers a total area of 350 square kilometers and stretches from latitude 35.22 to 34.99 north and longitude 3.52 to 3.77 west. The main river in the basin is the Amakran, which runs from the south of the study area to the north and into the Mediterranean, with an estimated length of 40 kilometers. The altitude of the area ranges from 49 to 1612 meters, and the slope extends from 0 to 63 degrees (Taher et al., 2023).

From a geological perspective, the Boudinar basin is situated on the internal boundary of the Riffian chain, and it is part of the Neogene basins that formed after the primary orogenic movements of the Rif. The basin comprises diverse geological regions that span from the Jurassic to the Quaternary. The sedimentary sequence of the Boudinar basin is traditionally classified into three principal series: the Upper Tortonian, Messinian, and lower Pliocene series (Ouahabi et al., 2007). The study area's vicinity has recorded around 770 seismic incidents between 1993 and 2023, according to the United States Geological Survey (USGS) (Fig. 4). These occurrences may have exacerbated the landslides in the Boudinar basin. However, this research's primary constraint is the unavailability of landslide inventory data, particularly for the validation phase. Consequently, Google Earth Pro was utilized to identify a total of 100 landslide incidents (Fig. 4 and . 5).

3. Materials and methods

3.1 Preparing landslide factor layers

A landslides susceptibility map was produced using nine parameters, which were classified using a weighted overlay analysis and the AHP technique. The rainfall map was generated using the inverse distance weighted (IDW) method, utilizing data from the Power Larc Project, supported by NASA, covering the period 2010-2021. The faults and lithology maps were digitalized based on the Boudinar geological map at a scale of 1/50000, provided by the geological survey of Morocco. The road map was digitalized from Google Earth. Additionally, the digital elevation model (DEM) obtained from the Earth Data (NASA) website was used to create topographic thematic layers, including aspect, slope, and elevation. Lastly, NDVI maps were created using Landsat 9 OLI data downloaded from the United States Geological Survey (USGS) (Table 2).

Topographic factors (Altitude, slope, aspect)

Elevation is a significant factor affecting the occurrence of landslides, as highlighted in several studies (Abedini and Tulabi, 2018; Alsabhan et al., 2022; Gupta et al., 2022; Wang et al., 2021) and is commonly utilized for LSM. Based on the elevation map depicted in Figure. 6a, the study area's altitude ranges from 49 m to 1612 m and has been divided into five categories. The regions with higher

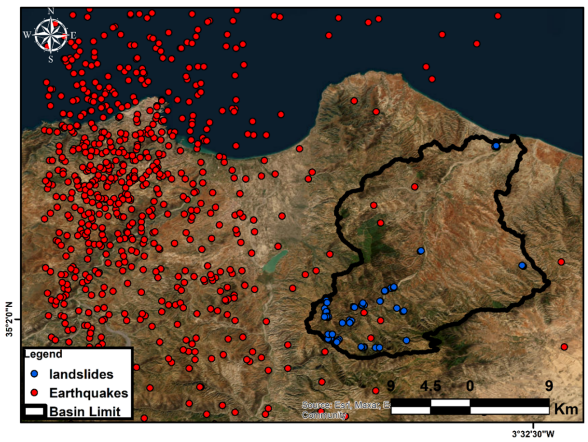

Figure 4. Spatial distribution of earthquakes from 1993 to 2023, and landslides inventory map of the Boudinar basin using Google Earth.

Figure 5. Example of landslide identified in study area using the Google Earth.

Table 2. Data information.

Data	Resolution / Scale	Free/Paid	Year	Source
DEM	12.5 × 12.5 m	Free	2007	https://search.asf.alaska.edu
Geological map	1/50000	Free	1984	Geological survey of Morocco
Landsat 9 OLI	30 × 30 m	Free	2022	https://earthexplorer.usgs.gov/
Rainfall	——-	Free	2010-2021	https://power.larc.nasa.gov/

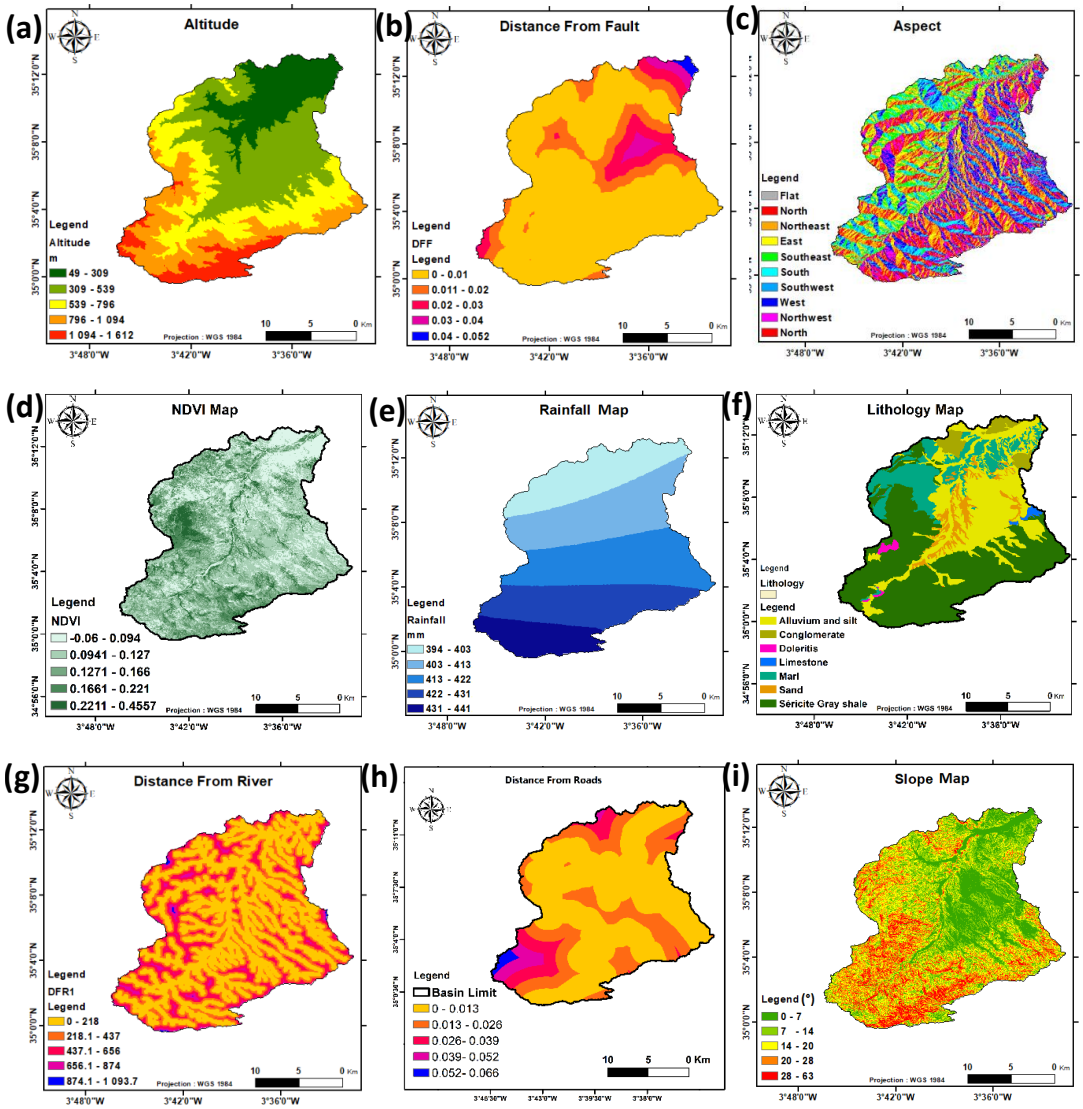

Figure 6. The parameters maps used in the current study.

elevations (assigned higher weights) are more susceptible to landslides compared to those with lower elevations (assigned lower weights).

Slope is regarded as a crucial topographic parameter for evaluating the potential of landslide occurrence in any area (Chang et al., 2022a; Saha et al., 2022). As shown in Figure. 6i, the slope gradients in the Boudinar basin range from 0 to 63 degrees. The lower slope gradients are primarily concentrated in the middle eastern and northeastern parts of the basin, while the higher gradients are found in the southern, southwestern, and southeastern regions. A higher score is assigned to areas with steeper slopes as they indicate a higher likelihood of landslides occurring.

The direction in which the slope faces, also known as aspect, is an important factor in assessing landslide susceptibility (Rehman et al., 2022; Saha et al., 2022). In the Boudinar basin, the aspect map (Fig. 6c) shows that areas facing south and west (higher score) receive more sunlight and have lower soil water content, while those facing north

(lower score) and east receive less sunlight and have higher soil water content (Saha et al., 2022; Wang et al., 2022). This information is crucial in determining the likelihood of landslides in different parts of the basin.

Distance from: Faults, Rivers, and Roads

Structural faults are commonly associated with landslide susceptibility due to tectonic activities (Jazouli et al., 2019; He et al., 2019). To create the distance from the faults map (Fig. 6b), the faults map was digitized from the 1/50000 scale geological map of Boudinar. The Euclidean distance tool in a GIS environment was utilized to generate distance categories, and the map was divided into five classes. Higher weight was assigned to areas with lower values, and vice versa. The river's activity can contribute to soil destabilization, thereby playing a role in the occurrence of landslides (Seddiki and Dehimi, 2022). Typically, it can be concluded that the probability of landslide occurrence decreases with increasing distance to rivers (Liu et al., 2022). In addition, the soil loss caused by river erosion has a serious impact on the stability of the slope. The slopes are eroded by the river and infiltrated by water, which leads to changes in internal stress and a greater probability of occurrence of collapses and landslides (Yuan et al., 2022). Similarly, the distance from rivers and roads (Fig. 5h) was calculated using the same tool, with areas closer to the river stream and roads being considered more susceptible to landslides (Jazouli et al., 2019; Kushal and Barman, 2022).

Lithology, NDVI and Rainfall

Lithology is a crucial factor in mapping landslide susceptibility, according to several studies (Kincal and Kayhan, 2022; Panchal and Shrivastava, 2022; Trinh et al., 2022). In the Boudinar basin (Fig. 6f), seven geology classes were identified. Marl, silt, and shale were assigned higher scores, while sand, dolerite, and conglomerate were assigned lower scores.

Vegetation density can affect landslide occurrence and soil erosion (He et al., 2019; Kincal and Kayhan, 2022). The normalized difference vegetation index (NDVI) is an important indicator of vegetation cover. In the study area (Fig. 6d), higher vegetation rates were observed in the middle west region. The NDVI value ranged from -0.06 to 0.45, with negative values indicating no vegetation cover. Higher NDVI values were given lower weight for landslide susceptibility mapping.

Precipitation is the most significant factor in landslides (He et al., 2019). Heavy storms and persistent rainfall can both trigger landslides. Loose soil in regions can lead to infiltration of rainwater on slopes and induce landslides. The annual rainfall map (2010-2021) for the Boudinar basin (Fig. 6e) shows that rainfall ranges from 394 mm to 441 mm. Higher rainfall areas were more susceptible to landslides (higher weights) than lower rainfall areas (lower weights).

3.2 Analytical hierarchy process method

The Analytical Hierarchy Process is a well-known approach for multi-criteria decision-making used to determine the weight of various criteria (Yamusa et al., 2022). It is a mathematical method that combines both qualitative and quantitative elements, as well as individual or group subjective judgments for sustainability (Yamusa et al., 2022). The AHP method simplifies complex issues through a layer-by-layer approach, calculating the weight of complex index systems through pairwise comparisons. The factors are compared against each other using a ranking threshold ranging from 1 to 9, as shown in Table 3 (Liu et al., 2022; Yamusa et al., 2022). The consistency ratio (CR) is determined by using the random index scale (Tabel 4). The consistency value for the matrix is acceptable if the consistency ratio value is less than 0.1 (Senapati and Das, 2022). However, having a CR greater than 0.1 (10%) requires a review of the decision matrix of the decision-makers (Yamusa et al., 2022).

$$\text{Consistency Ratio}(CR) = \frac{\text{Consistency Index } (CI)}{\text{Random Consistency Index}(RCI)}$$

where

$$CI = \frac{\lambda_{max} - n}{n-1} = \frac{8.939792 - 9}{9-1} = -0.007 < 0.1$$

$$CR = \frac{1.6466}{1.45} = 1.13$$

and

CW = Criteria Weight,

WSV = Weighted Sum Value, Ratio = WSV/CW

$\lambda_{max} = 8.939792$

For the current study, the pairwise normalized matrix determined the parameter's weight is shown in Table 5 and their sub-criteria weight of the AHP technique is shown in Table 6.

Table 3. The fundamental scale of Saaty (Saaty, 1990).

Intensity	1	3	5	7	9
Definition	Equal importance	Moderate importance	Strong importance	Very strong importance	Extreme importance

2, 4, 6, 8 intermediate values between the two adjacent judgments.

Table 4. The Random Index (RI) value (Saaty, 1990).

N	1	2	3	4	5	6	7	8	9
RI	0	0	0.58	0.89	1.12	1.25	1.32	1.40	1.45

Table 5. Pair-wise comparison matrix.

Rank	9	8	7	6	5	4	3	2	1			
	Lith	Slope	Rain	DFRo	DFR	NDVI	DFF	Elev	Asp	*CW*	*WSV*	Ratio
Lith	0.201	0.200	0.200	0.201	0.200	0.200	0.195	0.198	0.198	0.201	1.793	8.920
Slope	0.177	0.178	0.178	0.178	0.178	0.178	0.173	0.176	0.176	0.178	1.592	8.944
Rain	0.155	0.155	0.156	0.155	0.155	0.156	0.151	0.154	0.154	0.156	1.391	8.917
DFR	0.133	0.134	0.133	0.134	0.133	0.134	0.130	0.132	0.132	0.134	1.195	8.918
DFR	0.110	0.110	0.111	0.111	0.111	0.111	0.108	0.110	0.110	0.111	0.992	8.937
NDVI	0.088	0.089	0.089	0.088	0.089	0.089	0.086	0.088	0.088	0.089	0.794	8.921
DFF	0.066	0.066	0.066	0.067	0.067	0.067	0.065	0.053	0.066	0.065	0.583	8.969
Elev	0.044	0.045	0.044	0.044	0.044	0.045	0.043	0.044	0.044	0.044	0.397	9.023
Asp	0.022	0.022	0.022	0.021	0.022	0.022	0.021	0.022	0.022	0.022	0.196	8.909

Table 6. Normalized layer weight (NW) of subclasses.

Influencing factors	Class interval	Reclass	Overlay	NW%
Altitude (Alt) (m)	49 - 309	1	1	4
	309 - 539	2	2	
	539 - 796	3	3	
	796 - 1094	4	4	
	1094 - 1612	5	5	
Distance from fault (DFF)	0 - 0.01	1	5	6
	0.011 - 0.02	2	4	
	0.02 - 0.03	3	3	
	0.03 - 0.04	4	2	
	0.04 - 0.052	5	1	
Distance from river (DFR) (m)	0 - 218	1	5	12
	218 - 437	2	4	
	437 - 656	3	3	
	656 - 874	4	2	
	874 - 1093	5	1	
Lithology (Lith)	Alluvium and silt	-	4	20
	Conglomerate	-	1	
	Dolerites	-	1	
	Limestone	-	3	
	Marl	-	4	
	Sand	-	1	
	Sericite gray shale	-	4	
NDVI	-0.06 - 0.094	1	5	9
	0.0941 - 0.127	2	4	
	0.1271 - 0.166	3	3	
	0.1661 - 0.221	4	2	
	0.2211 - 0.4557	5	1	
Rainfall (Rai) (mm)	394 - 403	1	1	16
	403 - 413	2	2	
	413 - 422	3	3	
	422 - 431	4	4	
	431 - 441	5	5	
Slope (slp) (°)	0 - 7	1	1	18
	7 - 14	2	2	
	14 - 20	3	3	
	20 - 28	4	4	
	28 - 63	5	5	
Distance from roads	0 - 0.013	1	5	13
	0.013 - 0.026	2	4	
	0.026 - 0.039	3	3	
	0.039 - 0.052	4	2	
	0.052 - 0.066	5	1	
Aspect	Flat	1	2	2
	North	2	3	
	East	3	5	
	South	4	5	
	West	5	1	

4. Results and discussion

4.1 Landslide susceptibility map (LSM)

The AHP method was utilized to produce the LSM of the Boudinar basin, which was then classified into three categories: low, moderate, and high, as illustrated in Figure. 7. The high category, which accounts for 36% (88 km^2) of the study area (Table 7), is concentrated in the south and southeast. The findings indicate that slope, lithology, altitude, and NDVI are the most significant factors contributing to landslides. The moderate susceptible category, covering 69% of the total area (242 km^2) (Table 5), is situated in the central part of the Boudinar basin. The low class, with a susceptibility rate of 5% (18 km^2), is located in the north. It is important to note that the LSM outcome depends on the factors considered and their corresponding weightage (Panchal and Shrivastava, 2022). Regrettably, this is the first study conducted on LSM in the study area, and there are no previous studies available for comparison and validation. Nevertheless, uncertainties in the results may arise due to the impact of climate data, which is an essential factor with high weightage. The trend of hazardous phenomena used for susceptibility assessment can be related to the recovery period and recurrence possibility. If a particular hazardous event is occurring more frequently or with increasing intensity, it indicates a higher susceptibility to that event in the affected area. Considering these relationships is crucial for effective risk reduction, emergency management, and disaster response planning.

The NDVI and precipitation factors are dependent on climate change, which has a significant impact on landslides (Chang et al., 2022b; Jazouli et al., 2019), affecting their occurrence and magnitude. Increased precipitation altered vegetation dynamics, resulting in longer dry spells and drought. Vegetation plays a crucial role in slope stabilization by absorbing rainfall and reducing erosion (Zhang et al., 2015). However, climate change can weaken vegetation, reducing its ability to anchor soil and increasing landslide susceptibility. Considering the complex interactions between climate change, vegetation, and other factors is important when assessing landslide risks. Integrated land management strategies that focus on vegetation restoration, soil conservation, and slope stabilization are vital in mitigating landslide risks in a changing climate.

Table 7. The class percentage and area (km^2) of LSM.

Class	Low	Moderate	High
%	5	69	25
Area (km^2)	18	242	88

4.2 The validation of LSM

After the susceptibility map has been created, it must carry out the findings of the validation examination. Therefore, there are various methods for validating the LSM, including using a landslide inventory dataset (Byou, 2021). The field inventory of landslides posed a limitation in the validation step, which led us to utilize Google Earth for landslide inventory. While it may not be extremely accurate, it represents a better alternative than having no inventory at all. Therefore, 100 landslides were identified using Google Earth to validate the results. The Area Under the Receiver Operating Characteristic Curve (AUC-ROC) is a widely employed metric for assessing the overall performance of a classification model. It measures the model's capability to differentiate between positive and negative classes. A higher AUC-ROC value indicates superior discrimination and classification performance, reaching a maximum of 1, which signifies a perfect classifier. The AUC (Area Under the ROC curve) is crucial for validating the model's prediction performance (Kincal and Kayhan, 2022). For the current study, the AUC value reaches 0.65 (Fig. 8) indicating the model's satisfactory predictive quality. The obtained result confirms the findings of a comparative study conducted by Panchal and Shrivastava (2021) (Panchal and Shrivastava, 2021), indicating that the Analytic Hierarchy Process yielded the lowest accuracy, while the frequency ratio model yielded the highest accuracy. The prediction rate can be increased by varying the causative factors and their weightage (Panchal and Shrivastava, 2022).

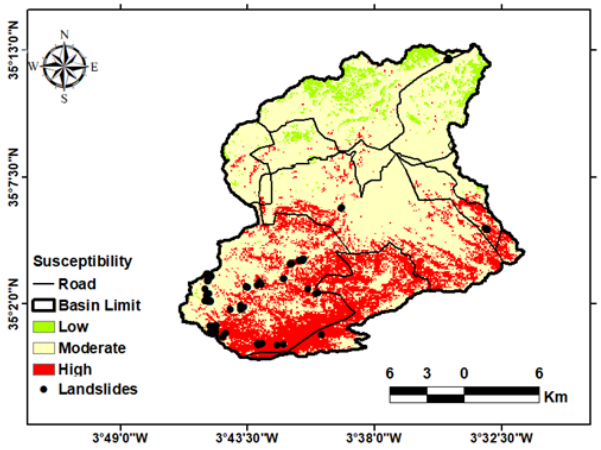

Figure 7. Landslide susceptibility map of the Boudinar basin.

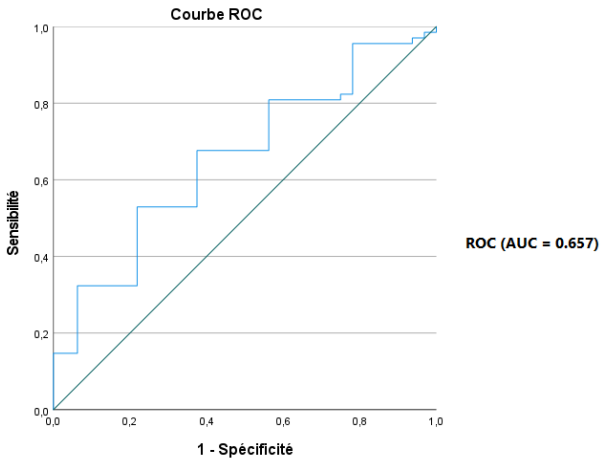

Figure 8. ROC curve validation of LSM using AHP method.

5. Conclusion and limitations

The Analytic Hierarchy Process and Geographic Information System were used to create a potential landslide susceptibility map. This study considered nine causative factors based on a literature review, including rainfall, lithology, slope, aspect, NDVI, distance from the fault, distance from the river, distance from the road, and elevation. AHP assigned weightage to the factors, revealing that rainfall, lithology, and slope are the primary contributors to landslide occurrence. To validate the result, a landslide inventory using Google Earth of 100 landslides was used as a positive sample. The resulting landslide hazard map was classified into three zones: low, moderate, and high. The study area showed that 25% of the land is in high-potential landslide zones, with a prediction rate of 0.657.

The factors used in this study are interconnected in influencing landslides, including rainfall, lithology, and slope. Therefore, heavy rainfall saturates soil, especially on steep slopes, leading to erosion and instability. Lithology affects water infiltration and retention, impacting soil stability. Steep slopes combined with specific lithological characteristics create landslide-prone conditions. These factors change dynamically both in space and time. Variations in precipitation amounts can be caused by seasonal rainfall patterns and extreme weather events. The frequency and intensity of rainfall are also impacted by long-term climate change, which directly affects landslip vulnerability. In addition, landslides are dramatically altered by human activity, including land-use changes, urbanization and deforestation. These alterations modify lithological characteristics, increase impermeable surfaces, and disrupt the equilibrium among these factors, often leading to heightened landslide susceptibility.

During our investigation, we have discerned a number of constraints, notably the quality and accessibility of data, which can exert a substantial influence on the outcomes of the AHP analysis, particularly with regard to soil and climate data. Additionally, it is worth noting that the study underscores the absence of antecedent research for purposes of comparison and validation. This absence of validation stemming from prior studies or real-world landslide occurrences renders it arduous to gauge the precision and dependability of the susceptibility classification generated by AHP. In this context, as a recommendation, to rectify the lack of soil data, and the lack of previous research for validation, it is advisable to suggest conducting field studies or surveys for landslides inventory, and soil sampling.

Finally, the LSM can be a valuable reference for concerned authorities, construction planners, and decision-makers. Finally, we highly recommend conducting further studies utilizing alternative methods, such as the frequency ratio model, in order to enhance the breadth and depth of the research findings.

Acknowledgments:
We would like to express our sincere gratitude to the reviewers for their valuable time and insightful comments on our article.

Authors contributions
Authors have contributed equally in preparing and writing the manuscript.

Availability of data and materials
The data that support the findings of this study are available from the corresponding author, upon reasonable request.

Conflict of interests
The authors declare that they have no known competing financial interests or personal relationships that could have appeared to influence the work reported in this paper.

References

Abedini M., Tulabi S. (2018) Assessing lnrf, fr, and ahp models in landslide susceptibility mapping index: a comparative study of nojian watershed in lorestan province, iran. *Environmental Earth Sciences* 77:1–13. DOI: https://doi.org/10.1007/s12665-018-7524-1.

Afzal N., Ahmad A., Shirazi S. A., Younes I., Ha L. T. T. (2022) Gis-based landslide susceptibility mapping using analytical hierarchy process: a case study of astore region, pakistan. *EQA-International Journal of Environmental Quality* 48:27–40. DOI: https://doi.org/10.6092/issn.2281-4485/12600.

Agrawal N., Dixit J. (2022) Assessment of landslide susceptibility for meghalaya (india) using bivariate (frequency ratio and shannon entropy) and multi-criteria decision analysis (ahp and fuzzy-ahp) models. *All Earth* 34:179–201. DOI: https://doi.org/10.1080/27669645.2022.2101256.

Akbar T. A., Ullah S., Ullah W., Ullah R., Sajjad R. U., Mohamed A., Khalil A., Javed M. F., Din A. (2022) Development and application of models for landslide hazards in northern pakistan. *Sustainability (Switzerland)* 14:1–17. DOI: https://doi.org/10.3390/su141610194.

Alsabhan A. H., Singh K., Sharma A., Alam S., Pandey D. D., Rahman S. A. S., Khursheed A., Munshi F. M. (2022) Landslide susceptibility assessment in the himalayan range based along kasauli-parwanoo road corridor using weight of evidence, information value, and frequency ratio. *Journal of King Saud University-Science* 34:101759. DOI: https://doi.org/10.1016/j.jksus.2021.101759.

Arjmandzadeh R., Rashvanlou V. Shafiei, Dabiri R., Almasi A. (2017) Satellite thermal surveys to detecting hidden active faults and fault termination, case study of quchan fault, ne iran. *Iranian Journal of Earth Sciences* 9:39–47.

Azarafza M., Azarafza M., Akgun H., Atkinson P. M., Derakhshani R. (2021) Deep learning-based landslide susceptibility mapping. *Scientific Reports* 11 (1): 1–16. DOI: https://doi.org/10.1038/s41598-021-03585-1.

Byou T. (2021) Evaluation of the landslide susceptibility map obtained by a gis matrix method: a case of al hoceima city (northern morocco). *SHS Web of Conferences* 119:04002. DOI: https://doi.org/10.1051/shsconf/202111904002.

Chang L., Zhang R., Wang C. (2022a) Evaluation and prediction of landslide susceptibility in yichang section of yangtze river basin based on integrated deep learning algorithm. *Remote Sensing* 14 (11) DOI: https://doi.org/10.3390/rs14112717.

Chang Z., Catani F., Huang F., Liu G., Meena S. R., Huang J., Zhou C. (2022b) Landslide susceptibility prediction using slope unit-based machine learning models considering the heterogeneity of conditioning factors. *Journal of Rock Mechanics and Geotechnical Engineering, xxxx.,* DOI: https://doi.org/10.1016/j.jrmge.2022.07.009.

Golian M., Teshnizi E. S., Parise M., Terzic J., Milanovic S., Vakanjac V. R., Mahdad M., Abbasi M., Taghikhani H., Saadat H. (2021) A new analytical method for determination of discharge duration in tunnels subjected to groundwater inrush. *Bulletin of Engineering Geology and the Environment* 80:3293–3313. DOI: https://doi.org/10.1007/s10064-021-02140-6.

Gupta N., Pal S. K., Das J. (2022) Gis-based evolution and comparisons of landslide susceptibility mapping of the east sikkim himalaya. *Annals of GIS* 28:359–384. DOI: https://doi.org/10.1080/19475683.2022.2040587.

Hamdouni I. El, Brahim L. A., Mahsani A. El, Abdelouafi A. (2022) The prevention of landslides using the analytic hierarchy process (ahp) in a geographic information system (gis) environment in the province of larache, morocco. *Geomatics and Environmental Engineering* 16:77–93. DOI: https://doi.org/10.7494/geom.2022.16.2.77.

Hashemi H., Yazdi A., TeshniziI E. Sharifi (2023) Mprovement of collapsing problematic soils on the sabzevar-mashhad railway route (northeast of iran) using traditional additives. *Nexo Revista Cientifica* 36:383–403. DOI: https://doi.org/10.5377/nexo.v36i03.16461.

He H., Hu D., Sun Q., Zhu L., Liu Y. (2019) A landslide susceptibility assessment method based on gis technology and an ahp-weighted information content method: a case study of southern anhui, china. *ISPRS International Journal of Geo-Information* 8 DOI: https://doi.org/10.3390/ijgi8060266.

Himmi M. (1994) General analysis of landslides in northern morocco: impact on the road network. *Proceedings of the 4th National Road Congress.*

Ibrahim M. B., Mustaffa Z., Balogun A. B., Indra S. H. H., Ain A. Nur (2022) Landslide's analysis and hazard mapping based on analytic hierarchy process (ahp) using gis, in lawas, sabah-sarawak. *IOP Conference Series: Earth and Environmental Science* 1064 (1) DOI: https://doi.org/10.1088/1755-1315/1064/1/012031.

Jazouli A. El, Barakat A., Khellouk R. (2019) Gis-multicriteria evaluation using ahp for landslide susceptibility mapping in oum er rbia high basin (morocco). *Geoenvironmental Disasters* 6 (1) DOI: https://doi.org/10.1186/s40677-019-0119-7.

KC D., Dangi H., Hu L. (2022) Assessing landslide susceptibility in the northern stretch of arun tectonic window, nepal. *CivilEng* 3 (2): 525–540. DOI: https://doi.org/10.3390/civileng3020031.

Kincal C., Kayhan H. (2022) A Combined method for preparation of landslide susceptibility map in izmir (turkiye). *Applied Sciences (Switzerland)* 12 (18) DOI: https://doi.org/10.3390/app12189029.

Kushal M., Barman S. D. (2022) Kodagu disaster (floods - emphasis on catchment fragmentation index and unscientific land usage) analysis using gis. *IOP Conference Series: Earth and Environmental Science* 1032 (1) DOI: https://doi.org/10.1088/1755-1315/1032/1/012036.

Leonardi G., Palamara R., Manti F., Tufano A. (2022) Gis-multicriteria analysis using ahp to evaluate the landslide risk in road lifelines. *Applied Sciences (Switzerland)* 12 (9) DOI: https://doi.org/10.3390/app12094707.

Liu Y., Yuan A., Bai Z., Zhu J. (2022) Gis-based landslide susceptibility mapping using frequency ratio and index of entropy models for she county of anhui province, china. *Applied Rheology* 32 (1): 22–33. DOI: https://doi.org/10.1515/arh-2022-0122.

Ouahabi F. Z. El, Martin S. Saint, Martin J. P. Saint, Moussa A. Ben, Conesa G. (2007) Messinian diatom assemblages from boudinar basin (northeastern rif, morocco). *Revue de Micropaleontologie* 50 (2): 149–167. DOI: https://doi.org/10.1016/j.revmic.2007.02.004.

Panchal S., Shrivastava A. K. (2021) A comparative study of frequency ratio, shannon's entropy and analytic hierarchy process (ahp) models for landslide susceptibility assessment. *ISPRS International Journal of Geo-Information* 10 (9) DOI: https://doi.org/10.3390/ijgi10090603.

——— (2020) Application of analytic hierarchy process in landslide susceptibility mapping at regional scale in gis environment. *Journal of Statistics and Management Systems* 23 (2): 199–206. DOI: https://doi.org/10.1080/09720510.2020.1724620.

——— (2022) Landslide hazard assessment using analytic hierarchy process (ahp): a case study of national highway 5 in india. *Ain Shams Engineering Journal* 13 (3): 101626. DOI: https://doi.org/10.1016/j.asej.2021.10.021.

Rahali H. (2019) Improving the reliability of landslide susceptibility mapping through spatial uncertainty analysis: a case study of al hoceima, northern morocco. *Geocarto International* 34 (1): 43–77. DOI: https://doi.org/10.1080/10106049.2017.1357767.

Rehman A., Song J., Haq F., Mahmood S., Ahamad M. I., Basharat M., Sajid M., Mehmood M. S. (2022) Multi-hazard susceptibility assessment using the analytical hierarchy process and frequency ratio techniques in the northwest himalayas, pakistan. *Remote Sensing* 14 (3): 1–31. DOI: https://doi.org/10.3390/rs14030554.

Reichenbach P., Rossi M., Malamud B. D., Mihir M., Guzzetti F. (2018) A review of statistically-based landslide susceptibility models. *Earth-Science Reviews* 180:60–91.

Saadat S., Ghoorchi M., Dabiri R. (2023) Extracting clay minerals with emphasis on bentonite in eastern iran, using landsat 8 and aster images. *Iranian Journal of Earth Sciences* 15 (3): 188–194. DOI: https://doi.org/10.30495/ijes.2023.1973739.1815.

Saaty T. L. (1990) How to make a decision: the analytic hierarchy process. *European Journal of Operational Research* 48 (1): 9–26. DOI: https://doi.org/10.1016/0377-2217(90)90057-i.

Saha A., Villuri V. G. K., Bhardwaj A. (2022) Development and assessment of gis-based landslide susceptibility mapping models using ann, fuzzy-ahp, and mcda in darjeeling himalayas, west bengal, india. *Land* 11 (10) DOI: https://doi.org/10.3390/land11101711.

Seddiki A., Dehimi S. (2022) Using gis combined with ahp for mapping landslide susceptibility in mila, in algeria. *International Journal of Design and Nature and Ecodynamics* 17 (2): 169–175. DOI: https://doi.org/10.18280/ijdne.170202.

Senapati U., Das T. K. (2022) Gis-based comparative assessment of groundwater potential zone using mif and ahp techniques in cooch behar district, west bengal. *Applied Water Science* 12 (3) DOI: https://doi.org/10.1007/s13201-021-01509-y.

Sheng M., Zhou J., Chen X., Teng Y., Hong A., Liu G. (2022) Landslide susceptibility prediction based on frequency ratio method and c5.0 decision tree model. *Frontiers in Earth Science* 10:1–14. DOI: https://doi.org/10.3389/feart.2022.918386.

Sun D., Chen D., Zhang J., Mi C., Gu Q., Wen H. (2023) Landslide susceptibility mapping based on interpretable machine learning from the perspective of geomorphological differentiation. *Land* 12 (5) DOI: https://doi.org/10.3390/land12051018.

Taher M., Mourabit T. (2022) The use of an elmi for measuring the movement of the trougout and the ajdir-imzouren faults-(north east of the rif) morocco—between 2017 and 2019. *Advances in Science, Technology and Innovation,* 95–99. DOI: https://doi.org/10.1007/978-3-030-73026-0$˙$24.

Taher M., Mourabit T., Etebaai I., Dekkaki H. C., Amine A., Abdelhak B., Errahmouni A., Azzouzi S. (2023) *Identification of Groundwater Potential Zones (GWPZ) Using Geospatial Techniques and AHP Method: a Case Study of the Boudinar Basin , Rif Belt (Morocco).* 17 (3): 83–106.

Trinh T., Luu B. T., Le T. H. T., Nguyen D. H., Tran T. Van, Nguyen T. H. Van, Nguyen K. Q., Nguyen L. T. (2022) A comparative analysis of weight-based machine learning methods for landslide susceptibility mapping in ha giang area. *Big Earth Data* 00 (00): 1–30. DOI: https://doi.org/10.1080/20964471.2022.2043520.

Trisnawati D., A. S. Najib Hidayatillah, Robbany A. Z., Pellokila Y. A. L. (2022) Comparative study of determination of landslide susceptibility based on weighting methods and analytical hierarchy processes in pringapus, east ungaran. *IOP Conference Series: Earth and Environmental Science* 1039 (1): 012024. DOI: https://doi.org/10.1088/1755-1315/1039/1/012024.

Wang H., Zhang L., Yin K., Luo H., Li J. (2021) Landslide identification using machine learning. *Geoscience Frontiers* 12 (1): 351–364. DOI: https://doi.org/10.1016/j.gsf.2020.02.012.

Wang Z., Ma C., Qiu Y., Xiong H., Li M. (2022) Refined zoning of landslide susceptibility: a case study in enshi county, hubei, china. *International Journal of Environmental Research and Public Health* 19 (15) DOI: https://doi.org/10.3390/ijerph19159412.

Yamusa I. B., Ismail M. S., Tella A. (2022) Highway proneness appraisal to landslides along taiping to ipoh segment malaysia, using mcdm and gis techniques. *Sustainability (Switzerland)* 14 (15) DOI: https://doi.org/10.3390/su14159096.

Yuan X., Liu C., Nie R., Yang Z., Li W., Dai X., Cheng J., et al. (2022) A comparative analysis of certainty factor-based machine learning methods for collapse and landslide susceptibility mapping in wenchuan county, china. *Remote Sensing* 14 (14) DOI: https://doi.org/10.3390/rs14143259.

Zhang L., Wang J., Bai Z., Lv C. (2015) Effects of vegetation on runoff and soil erosion on reclaimed land in an opencast coal-mine dump in a loess area. *Catena* 128:44–53. DOI: https://doi.org/10.1016/j.catena.2015.01.016.